arXiv:hep-ex/0110075 v1 30 Oct 2001

The $J^{PC} = 1^{-+}$ hunting season at VES

Valery Dorofeev (for VES Collaboration [1])

Department of Hadron Physics, IHEP, Protvino, Russia, 142284

Abstract. We present preliminary results of study of the $\eta\pi^-$, $\eta'\pi^-$ and $b_1\pi$-systems produced in the $\pi^- Be$-interaction at 28 GeV/c. $J^{PC} = 2^{++}$ and 1^{-+}-waves resulted from the PWA have been fitted in each system separately to establish the nature of the 1^{-+}-wave. A hypothesis of the 1^{-+}-wave resonant nature in the $\eta\pi^-$ and $\eta'\pi^-$ has no statistically significant preference over the non-resonant one. The $b_1\pi$-system analysis confirms the results of the 37 GeV/c-beam data analysis in favor of the resonant treatment of the bump at $1.6GeV$.

INTRODUCTION

At present several groups have evidence for 1^{-+} meson production, which is forbidden for ordinary quarkonia and hence might be a good candidate for a hybrid [1], [2]. The $\pi_1(1400)$-meson shows up in the $\eta\pi$ final state in two experiments [3],[4],[5]. VES group found that the results of the $\eta'\pi^-$ and $b_1\pi$-system Partial-Wave Analysis(PWA) at $37GeV/c$ agree with the production of the higher mass $\pi_1(1600)$ [6], evidence for which in the $\eta'\pi^-$ has been also confirmed by E852 at BNL [7]. A broad bump observed by VES in the 1^{-+}-wave intensities of the $\eta'\pi$, $b_1\pi$, $\rho\pi$ at $1.6GeV$ was assumed to be a single object. The resonant nature results from the analysis of the $J^{PC} = 2^{++}$ and 1^{-+}-waves in the $\omega\pi^-\pi^0$ [8].

A data sample was collected in the 1996 data run at VES spectrometer exposed by the $28GeV/c$ momentum π^--meson beam. A detailed description of setup can be found elsewhere [9]. Over 5×10^8 triggers were recorded during the data taking period, which is ~ 2.5 more than at $37GeV/c$. A trigger is an event with at least two charged tracks from the beam interaction moving in the beam direction and falling into the spectrometer aperture. Events of the studied final states production form subsets of reaction $\pi^- Be \to \pi^+ 2\pi^- + k\pi^0(\eta) + Be$, where $k = 1, 2$. To select events of this reaction the following criteria were applied to the reconstructed events:

- 3 reconstructed tracks should form the $\pi^+\pi^-\pi^-$-system;
- an interaction vertex must be inside the target;
- we require for 2-4 γ-clusters in the calorimeter;

[1] Amelin D.V., Dorofeev V.A., Dzhelyadin R.I., Gouz Yu.P., Kachaev I.A., Karyukhin A.N., Khokhlov Yu.A., Konoplyannikov A.K., Konstantinov V.F., Kopikov S.V., Kostyukhin V.V., Matveev V.D., Nikolaenko V.I., Ostankov A.P., Polyakov B.F., Ryabchikov D.I., Solodkov A.A., Solovianov O.V., Zaitsev A.M.

- a 2γ-system with mass closest to the mean $\pi^0(\eta)$-meson mass within $30(78)MeV$ is identified as the $\pi^0(\eta)$-meson. A 1C-fit to the $\pi^0(\eta)$ mass is applied to the identified $\gamma\gamma$ pairs;
- total visible energy E_{tot} must satisfy the following in-equation: $25GeV < E_{tot} < 30GeV$.

STUDY OF THE $\eta\pi^-$-SYSTEM

A decay chain $\eta \to \pi^+\pi^-\pi^0$, $\pi^0 \to 2\gamma$ was chosen for the $\eta\pi^-$ production study. A clear peak of the η-meson corresponding to the $\eta\pi^-$ production is observed in an invariant mass spectrum of the $\pi^+\pi^-\pi^0$-system in fig. 1a. The shape of the peak is parametrized with a sum of two Gaussian functions and resolution of the narrow one is equal to $6MeV$. Shown in fig. 1b is the invariant mass distribution of the $\pi^+2\pi^-\pi^0$ for events from the η region ($530 < M_{\pi^+\pi^-\pi^0} < 566MeV$) with superimposed plot for sidebands ($502 < M_{\pi^+\pi^-\pi^0} < 520MeV$ and $576 < M_{\pi^+\pi^-\pi^0} < 594MeV$) which are used for the background estimation. The background subtracted $\eta\pi^-$ invariant mass spectrum (fig. 1c) shows a dominant $a_2(1320)$-meson production with a small bump near $M_{\eta\pi^-} = 1GeV$ of a possible $a_0(980)$-meson production.

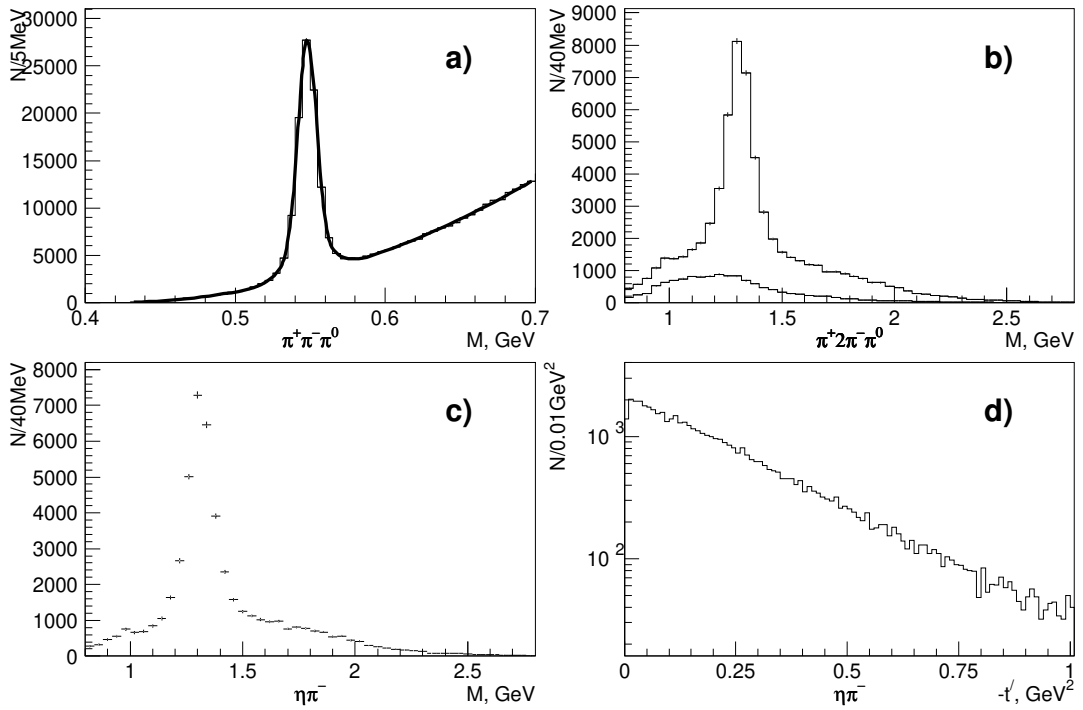

FIGURE 1. Effective mass of the $\pi^+\pi^-\pi^0$ a), $\pi^+2\pi^-\pi^0$ b) and $\eta\pi^-$ c). $-t'$ distribution d).

A negative value of the invariant four-momentum-transfer between the beam and the $\eta\pi^-$ squared $-t'$-distribution in fig. 1d shows the characteristic features of the projective

wave production. Here $t' = t - t_{min}$, where t_{min}- is a minimum transfer squared for a given $\eta\pi^-$ mass.

The $\eta\pi^-$-system PWA

We applied the PWA procedure to expand the data in terms of the partial waves. An event is considered in the spirit of the isobar model [10] as a production process followed by a chain of the subsequent decays into the $\eta\pi^-$ and $\eta \to \pi^+\pi^-\pi^0$. The production process of the $\eta\pi^-$ is assumed to be described by a rank one density matrix for each naturality [11]. An event probability for each naturality is equal to an average over possible non-interfering $\pi^+\pi_i^-\pi^0$ combinations N_{comb} of a product: $P_{ev} = \frac{1}{N_{comb}} \sum_i P_i D_i(m_{3\pi}) G_i(m_{3\pi})$ due to presence of two π^-'s, where: D_i - is a probability of the $\eta \to \pi^+\pi_i^-\pi^0$ decay which corresponds to the decay Dalitz-plot distribution, G_i - is the η-meson shape parameterization being used to take into account the $\pi^+\pi_i^-\pi^0$ mass resolution. Here P_i is an expansion squared of the product of the two pseudo-scalar production and decay amplitudes in terms of the partial wave decay amplitudes. The decay amplitudes are defined by the following set of quantum numbers $J^P M^\eta$, where J stands for a total angular momentum and is equal to an orbital momentum L in the system of two pseudo-scalars. With P we denote parity, M - an absolute value of the J_z projection. Here η is exchange naturality. The decay amplitude is parametrized with spherical harmonics [12] multiplied by a breakup momentum involved in the L-th degree. Under the assumption about the rank of the density matrix the production amplitudes are denoted as: L_0 for the $M = 0$ and L_η for the $M = 1$ waves.

The complex production amplitudes are determined from the extended maximum likelihood fit [13].

A wave set includes 3 subsets of partial waves non-interfering with each other. The first is composed of waves with negative naturality, the second - with positive one and a subset made of a single wave FLAT which describes the background in the $\pi^+ 2\pi^-\pi^0$-system.

The ambiguous solutions [14] were found by repeating 100 times the fit from the random starting values of the fit parameters.

50300 events in the range $0.8 < M(\pi^+ 2\pi^-\pi^0) < 2.4 GeV$, $|t'| < 1 GeV^2$, with the mass of at least a single $\pi^+\pi^-\pi^0$ combination in the η region or the sidebands were subjected to the PWA. The PWA has been carried out independently in each of the $40 MeV$ bins. To make the data set cleaner the following additional cuts were applied: $\cos\Theta^{hel}_{\pi^0} < 0.8$ and the track angular separation in projections $\Delta AX(AY) > 10(6) mrad$, where $\Theta^{hel}_{\pi^0}$ is the π^0 polar angle in the overall CM helicity reference frame.

In fig. 2 are shown predicted by the PWA fit acceptance-corrected wave intensities and a relative phase between the P_+ and D_+ waves as a function of the $\eta\pi^-$ mass. With a thick line is shown a range of possible ambiguous solutions and with a thin one the maximum extent of errors.

The intensities of the S and P waves with the negative naturality are small and consistent with zero in all the $M_{\eta\pi^-}$ range. The D_0 wave has a non-zero contribution in the $M_{\eta\pi^-} > 2 GeV$. We found a significant D_- intensity in the whole mass range of

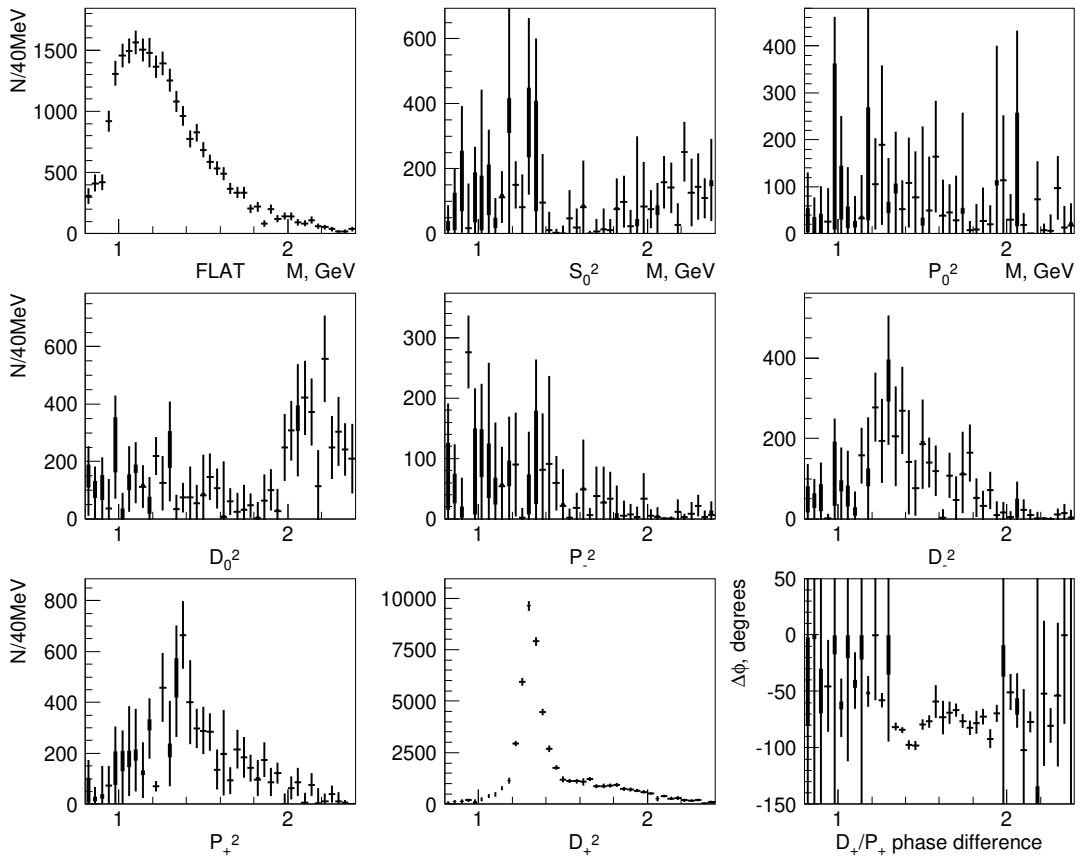

FIGURE 2. The $\eta\pi^-$ wave intensities and the D_+/P_+ relative phase.

unclear nature.

The D_+-wave is the dominantly produced wave in the $\eta\pi^-$, where a huge peak corresponding to the $a_2(1320)$ production is observed. A broad bump with a spike at $M_{\eta\pi^-} = 1.4GeV$ is observed in the P_+. The spike might results from the fit quality worsening in the $a_2(1320)$ region and where one should notice the increase of errors. A sign ambiguous relative phase shows a rapid motion in the $a_2(1320)$ region.

We have tried also to include the waves with the orbital momentum higher than 2 and the waves with $M > 1$, but they were found to be not significant. The quality of the fit is controlled by comparison of distributions of variables which describe the $\eta\pi^-$-system for the experimental and Monte-Carlo data. The Monte-Carlo events were generated according to the described above model with the values of the production amplitudes resulted from the best fit solution in a mass bin.

The $\eta\pi^-$-system mass-dependent fit

In order to establish the nature of the P_+-wave we have carried out a combined mass-dependent(MD) fit of the expected production amplitudes to the P_+ and D_+ resulted from the PWA in the whole mass range. Fitted with the χ^2 method are the D_+ and P_+ intensities and the real and imaginary parts of the production of both amplitudes with the corresponding errors in each mass bin.

We assume two general production manners of a resonant and a non-resonant type. The resonant amplitude is parametrized with a Breit-Wigner form:

$$A_R = \frac{m_0\sqrt{\Gamma_0\Gamma_f}}{m_0^2 - m^2 - im_0\Gamma_{tot}}, \qquad \Gamma_f = BR_f\Gamma_0\frac{m_0}{m}\frac{q}{q_0}\left[\frac{B_L(q)}{B_L(q_0)}\right]^2$$

where: m - the $\eta\pi$ mass, m_0 - a resonance mass, Γ_0 - a nominal width, Γ_f - a partial width in the final channel, Γ_{tot} - a total width, $q(q_0)$ - a breakup momentum of the $\eta\pi$ with the $m(m_0)$ mass, $B_L(q)$ - a barrier factor [15], BR_f - a branching ratio into the f-th final state.

By the notion background we just mean the non-resonant production manner without going into the nature of the process. The main difference of the background type from the resonant one is absence of phase motion. The background amplitude is parametrized with the following free form $A_B = LIPS_l \times (m - m_t)^{\alpha}\exp(-\beta(m - m_t))$, where: $LIPS_l(m)$ - a phase space, m_t - a threshold mass, α and β are shape parameters.

A procedure of the wave construction from the objects is in the following. At first a wave is formed of evident structures such as the $a_2(1320)$ in the D_+-wave. If there are no such objects we take an object of any production type arbitrarily. After doing the fit to thus constructed wave we then necessarily try to describe the data with the object of the alternative type. At the next steps we add consistently another objects of both types to both waves until we will succeed in the description of the wave intensities and their interference in the whole mass region. All objects are added coherently with their own mass-independent phase. The parameters of the MD fit are: the mass, width and the number of the resonance events, the shape parameters and the number of the background events, the phase relative to a reference object.

TABLE 1. Comparison of the MD fit variants

D_+ bkg	a_2'	P_+ bkg	π_1	χ^2/NDF
+		+		244/149
	+	+		422/149
+			+	224/149
	+		+	219/149
+		+	+	176/145
+		+	E852	187/147

To begin with we have fitted the $a_2(1320)$ Breit-Wigner to the D_+ intensity and failed to describe the D_+ wave at masses $> 1.5GeV$. Then we have applied the described above

procedure. At first the D_+ was fitted to a sum of the $a_2(1320)$ and the background and the P_+ to the background. The second fit was carried out with the D_+ wave background replaced by the resonance, which will be called further as an a_2'-meson for convenience. There have just been reported the evidence for the $a_2(1750)$ [16]. The next steps were to fit the P_+ wave to the resonance, called a $\pi_1(1400)$. The evidence for it have been reported by E852 and CBAR groups [3], [4], [5] and which production did not contradict to VES results [17]. The results of the MD fits in the case, when the D_+ has been fitted to a sum of the $a_2(1320)$ and the background and the P_+ to the background or to the π_1 are shown in fig. 3 with thick solid and dashed curves respectively.

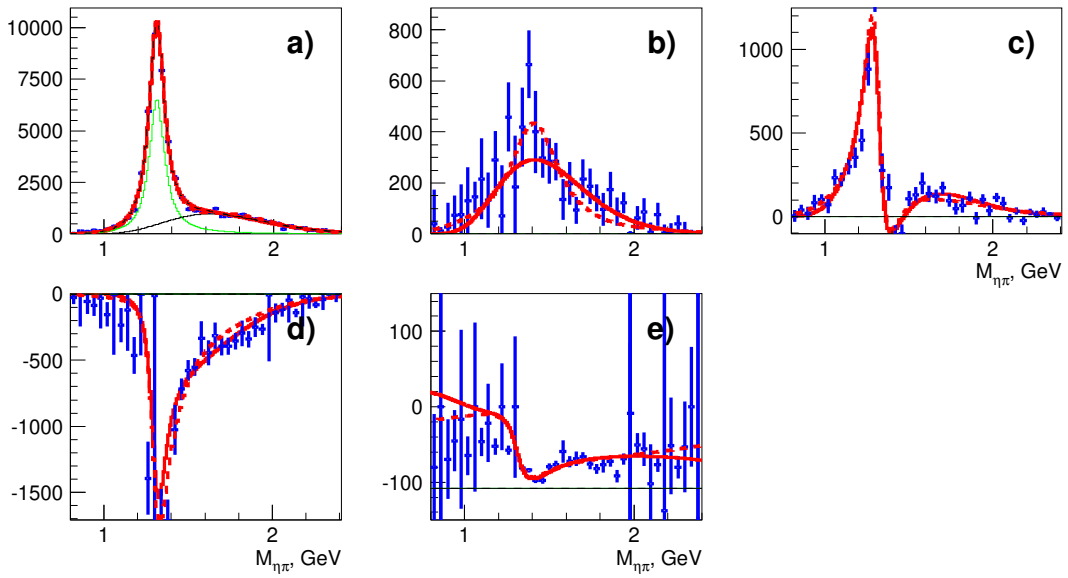

FIGURE 3. The $\eta\pi^-$ D_+ a) and P_+ b) intensities. The real c) and imaginary d) parts of D_+P_+ product. The D_+/P_+ relative phase e). The smooth curves are the MD fit results.

The summary of the MD fit results are presented in tab. 1. The objects which make up the fitted partial waves are marked by the plus sign in a row. A χ^2 over the number of degrees of freedom of the corresponding MD fit is shown in the fifth column.

From the comparison of the first four rows one can conclude that there are no statistically significant difference between a single resonant and non-resonant object description of the P_+.

The fits of the P_+ to a sum of the π_1 and the background are shown in the last two rows. A fit with free π_1 parameters resulted in the following values: $M_{a_2(1320)} = 1316 \pm 1 MeV$, $\Gamma_{a_2(1320)} = 113 \pm 3 MeV$, and $M_{\pi_1} = 1316 \pm 12 MeV$, $\Gamma_{\pi_1} = 287 \pm 25 MeV$. The quoted errors are statistical only. Statistical significance is nearly the same as for the fit with the π_1 parameters fixed to the values reported by E852 [3]. A closeness of the π_1 mass to the $a_2(1320)$ mass may indicate that there is an underestimated influence of the $a_2(1320)$ on the P_+.

STUDY OF THE $\eta'\pi^-$-SYSTEM

A decay chain $\eta' \to \eta\pi^+\pi^-$, $\eta \to 2\gamma$ was chosen for the $\eta'\pi^-$ production study. A clear peak of the η' corresponding to the $\eta'\pi^-$ production is observed in the invariant mass spectrum of the $\eta\pi^+\pi^-$ in fig. 4b. Shown in fig. 4c is the invariant mass distribution of the $\eta\pi^+2\pi^-$ for events from η' region ($940 < M_{\eta\pi^+\pi^-} < 976 MeV$) with superimposed plot for the η' sidebands ($912 < M_{\eta\pi^+\pi^-} < 930 MeV$ and $986 < M_{\eta\pi^+\pi^-} < 1004 MeV$) which are used for the background estimation. The background subtracted $\eta'\pi^-$ invariant mass spectrum (fig. 4d) shows a clear $a_2(1320)$ peak and a broad large bump at $M_{\eta\pi^-} = 1.6 GeV$, which strongly differs from the corresponding distribution of the $\eta\pi^-$.

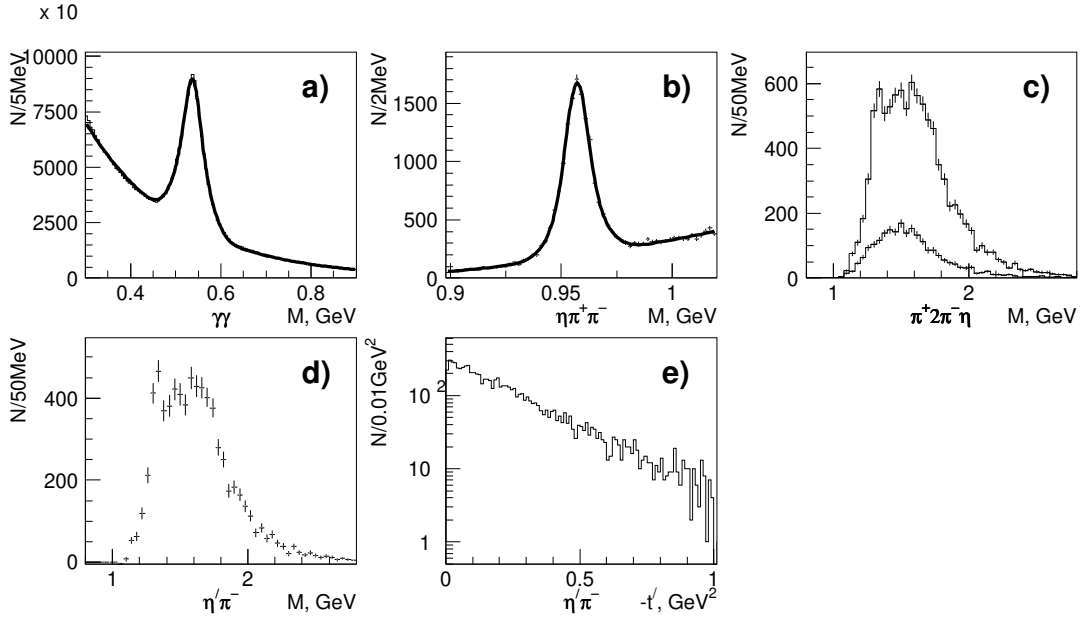

FIGURE 4. Effective mass of the $\gamma\gamma$ a), $\eta\pi^+\pi^-$ b), $\eta\pi^+2\pi^-$ c) and $\eta'\pi^-$ d). $-t'$ distribution e).

A $-t'_{\eta'\pi^-}$ distribution in fig. 4e shows characteristic features of the projective wave production like for the $\eta\pi^-$.

10700 events in the range $1.15 < M(\eta\pi^+2\pi^-) < 2.15 GeV$, $|t'| < 1 GeV^2$, with the mass of at least a single $\eta\pi^+\pi^-$ combination in the η'-meson region or the sidebands were subjected to the PWA. The PWA has been carried out independently in each of the $50 MeV$ wide bins.

We have applied the same procedure as for the $\eta\pi^-$-system PWA, described in the appropriate section. In fig. 5 are shown predicted by the PWA fit acceptance-corrected wave intensities and a phase difference of the P_+ and D_+ as a function of the $\eta'\pi^-$ mass. With a thick line is shown a range of possible ambiguous solutions and with a thin one the maximum extent of errors.

The intensities of the negative naturality waves are small and nearly consistent with zero in all the $M_{\eta'\pi^-}$ range. The D_0 wave only shows some non-negligible contribution in the regions $1.4 \div 1.6 GeV$ and $> 1.9 GeV$.

The $a_2(1320)$ peak is observed in the D_+ intensity. But contrary to the $\eta\pi^-$-system

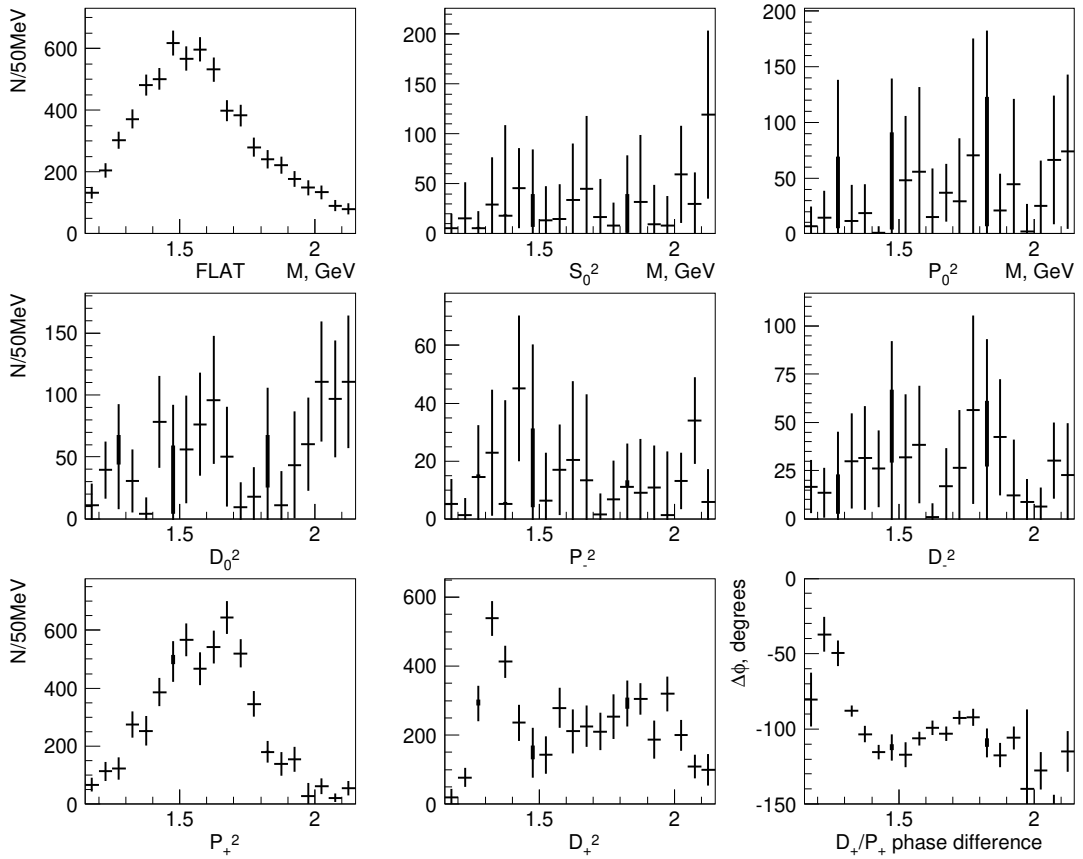

FIGURE 5. The $\eta'\pi^-$ wave intensities and the D_+/P_+ relative phase.

behavior this wave shows a broad structure in the region $M_{\eta'\pi^-} > 1.5GeV$. The rate of this high mass production relative to the $a_2(1320)$ is larger for the $\eta'\pi^-$ than for $\eta\pi^-$.

A broad bump of a $\sim 350MeV$ width is observed in the P_+ at $M_{\eta'\pi^-} = 1.6GeV$. A sign ambiguous relative phase shows a rapid motion in the $a_2(1320)$ mass region.

We have tried also to include the waves with the orbital momentum higher than 2 but they were found to be not significant. The quality of the fit is controlled by comparison of distributions of variables which describe the $\eta'\pi^-$-system for the experimental and Monte-Carlo data.

To establish the nature of the P_+-wave we have carried out the MD fit following the procedure which had been applied for the $\eta\pi^-$ study. The D_+ partial wave amplitude was parametrized with a sum of the $a_2(1320)$ Breit-Wigner function and the background or an a_2'. This additional object was included to describe the broad bump in the region $M_{\eta'\pi^-} > 1.5GeV$. The P_+ partial wave was parametrized with the background or with the $\pi_1(1600)$. The indication to the possible resonance nature of the bump at $1.6GeV$ was reported by our group as a result of the $\eta'\pi^-$ PWA at $37GeV/c$ [6]. Later the observation of the resonance have been reported by E852 [7]. The result of the MD fit in the case, when the D_+ is fitted to a sum of the $a_2(1320)$ and the a_2' and the P_+ to the resonance

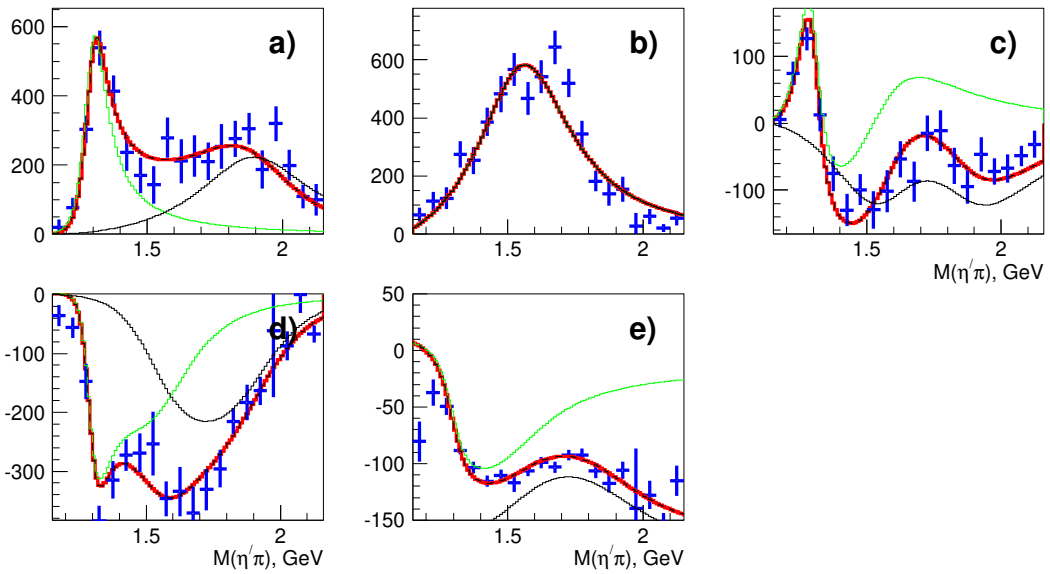

FIGURE 6. The $\eta'\pi^-$ D_+ a) and P_+ b) intensities. The real c) and imaginary d) parts of D_+P_+ product. The D_+/P_+ relative phase e). The smooth curves are the MD fit results.

only is shown in fig. 6.

We have found no statistically significant preference of the fit with the P_+ saturated with the resonant over the non-resonant description. In the case of the P_+ partial wave amplitude parameterization with a sum of the resonance and the background the statistical significance is larger than in the previous cases. However the $a_2(1320)$ width was found to be somewhat larger than it could be expected from the resolution study. In the cases, when the D_+ is composed of the $a_2(1320)$ and a a_2', while the P_+ includes the π_1, the a_2' mass was found to be somewhat $1.8 \div 1.9 GeV$ and the width $0.4 \div 0.5 GeV$, while one might expect to find the same parameters as for the $a_2'(1750)$.

The above consideration of results prevents us from drawing the unambiguous conclusion about the nature of the P_+-wave in the $\eta'\pi^-$.

STUDY OF THE $\omega\pi^-\pi^0$-SYSTEM

A decay mode $\omega \to \pi^+\pi^-\pi^0$ was chosen for the $\omega\pi^-\pi^0$ production study. A clear peak of the ω meson corresponding to the $\omega\pi^-\pi^0$ production is observed in the invariant mass spectrum of the $\pi^+\pi^-\pi^0$ in fig. 7a. Shown in fig. 7b is the invariant mass distribution of the $\pi^+2\pi^-2\pi^0$ for events from the ω region ($758 < M_{\pi^+\pi^-\pi^0} < 808 MeV$) with superimposed plot for the ω sidebands ($684 < M_{\pi^+\pi^-\pi^0} < 719 MeV$ and $846 < M_{\pi^+\pi^-\pi^0} < 871 MeV$) which are used for the background estimation. The background subtracted $\omega\pi^-\pi^0$ invariant mass spectrum (fig. 7c) shows an $a_2(1320)$ shoulder and a broad large bump at $M_{\omega\pi^-\pi^0} = 1.8 GeV$.

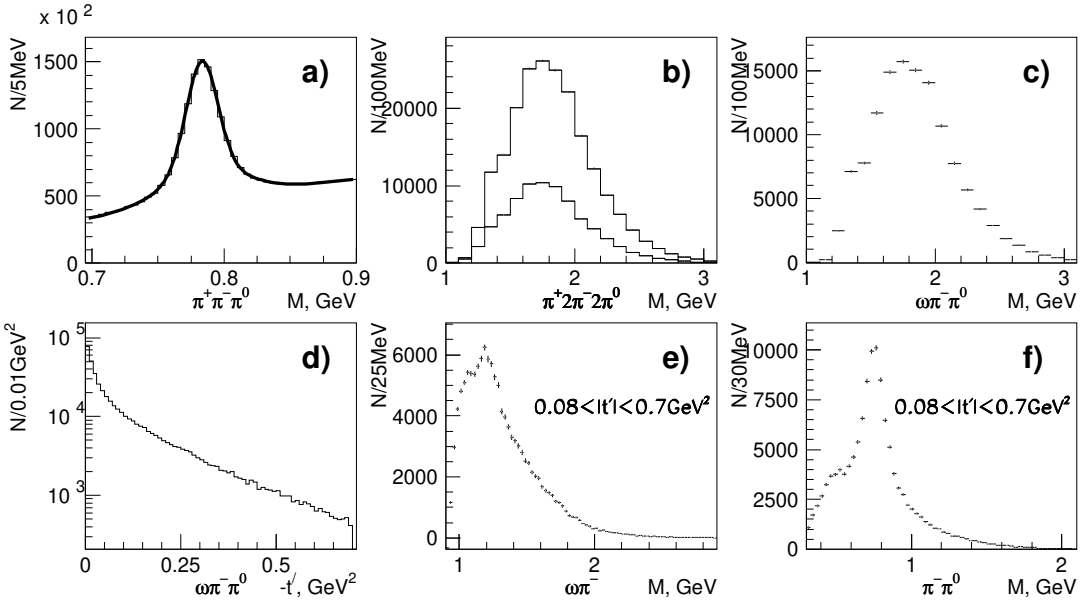

FIGURE 7. Effective mass of the $\pi^+\pi^-\pi^0$ a), $\pi^+2\pi^-2\pi^0$ b) and $\omega\pi^-\pi^0$ c). $-t'$ distribution d). Effective mass of the $\omega\rho^-$ e) and $\pi^-\pi^0$ f) from the $\omega\pi^-\pi^0$ for $0.08 < |t'| < 0.7GeV^2$.

A $-t'_{\omega\pi^-\pi^0}$-distribution in fig. 7d shows a sharp peak in the low $|t'| < 0.08GeV^2$ (LT) region, corresponding to the coherent production on a nucleus, which flattens in the high $|t'|$ region ($0.08 < |t'| < 0.7GeV^2$) and which will be called further the HT. This behavior in the HT-region corresponds to the incoherent production on a nucleon. The projective wave production dominates in the HT-region. Therefore we have divided a data sample into the LT- and HT-sets, which were analyzed separately. A large ρ^--meson peak is observed in the invariant mass spectrum of the $\pi^-\pi^0$, produced with the ω(see fig. 7f). This means the dominant production of the $\omega\rho^-$. There is a peak of the $b_1(1235)^-$-meson in the $\omega\pi^-$ invariant mass spectrum shown in fig. 7e, corresponding to the $b_1(1235)\pi$ production. The same is for the $b_1(1235)^0$.

A PWA of 284000 events in the range $1.2 < M(\pi^+2\pi^-2\pi^0) < 3GeV$, $0.08 < |t'| < 0.7GeV^2$, $\max_{\pi^\pm}(\cos\Theta^{hel}) < 0.92$ with the mass of at least one $\pi^+\pi^-\pi^0$-combination in the ω region or in the sidebands has been carried out. Here Θ^{hel} is a track polar angle in the overall helicity CM reference frame. Events in each of the $50MeV$ or $100MeV$ wide bins were fitted separately. The Illinois method [11] was used in the PWA, however with an important improvement. We added the possibility to restrict a rank of the density matrix [18]. The partial waves are denoted by the $J^PM^\eta LS(isobar - bachelor)$, where S stands for a total spin in the isobar-bachelor system. The partial waves of the $\omega\rho^-$, $b_1(1235)\pi$, $\rho_3(1690)\pi$, $\rho_1(1450)\pi$ are included in the wave set. The results of the PWA are consistent with our previous analysis of the $\omega\pi^-\pi^0$ at $37GeV/c$ [19]. A $2^+1^+S2(\omega\rho)$ shown in fig. 8a was found to be a dominant wave with a clear $a_2(1320)$ peak and a broad bump at $M_{\omega\pi^-\pi^0} = 1.7GeV$. A significant $1^-1^+S1(b_1\pi)$ wave shown in fig. 8b is observed with a broad bump at $M_{\omega\pi^-\pi^0} = 1.6GeV$, which is in the maximum $\sim 15\%$ of the $a_2(1320)$ peak height. The important feature of the combined 2^+ and 1^- wave

behavior demonstrated in fig. 8c is a region bounded to $1.5 < M_{\omega\pi^-\pi^0} < 2GeV$, where the coherence is significantly non-zero. It should be noticed in fig. 8f an 80° rise of the 1^--wave phase relative to the 2^+-wave phase right in this region and which may be attributed to a 1^- resonance.

The MD fit has been carried out to establish the origin of the 1^-1^+-wave in the $b_1\pi$. The high intensity $2^+1^+S2(\omega\rho)$ was selected to be a reference wave. The fit has been done in the same way like the $\eta\pi^-$ fit. However absence of unambiguous knowledge about the nature of the bump at $M_{\omega\pi^-\pi^0} = 1.7GeV$ and an extension of the density matrix rank to three in the PWA requires inclusion of additional fitting parameters in the MD fit. The naïve model is to describe the 2^+ wave by a sum of the $a_2(1320)$ Breit-Wigner and something, which has a form of the bump at $1.7GeV$, while the 1^- may be constructed from a broad incoherent background and from a resonance, which is coherent to the 2^+ bump.

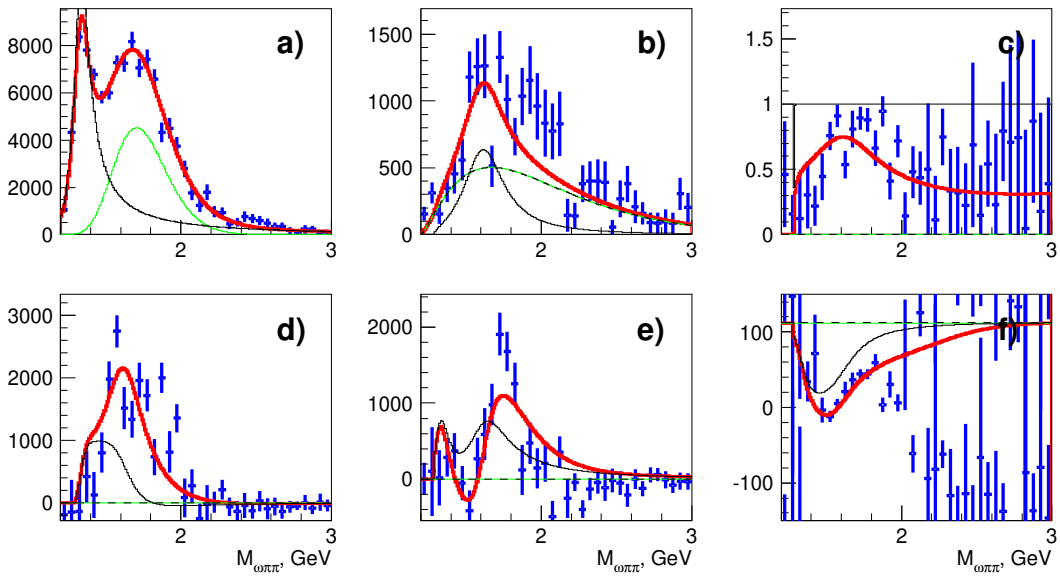

FIGURE 8. The $2^+1^+S2(\omega\rho)$ a) and $1^-1^+S1(b_1\pi)$ b) intensities. A coherence parameter c) [11]. The real d) and imaginary e) parts of their non-diagonal ρ-matrix element. The 1^- phase relative to 2^+ f). The smooth curves are the MD fit results.

The fit describes the interference pattern satisfactorily as seen in fig. 8. We have tried another hypotheses: to fit the 1^- wave to a partially coherent background or to make up the 2^+ wave from a a_2' in addition to the $a_2(1320)$. However we failed to find qualitatively better solution. The data are consistent with the resonant description of the $1^-1^+S1(b_1\pi)$ with the mass $1.6GeV$ and the width $0.33GeV$.

CONCLUSIONS

We have carried out the PWA of the $\eta\pi^-$, $\eta'\pi^-$, $b_1\pi$ systems produced in π^-Be interaction at $28GeV/c$.

We have tried to understand the nature of the observed partial waves in each system by the fit to the resonant and non-resonant description.

- We observed the P_+ in the $\eta\pi^-$ which exhibits the phase motion with respect to the D_+ in the coherent model. We could not unambiguously establish the nature of the P_+ in the $\eta\pi^-$.
- The production of the $\eta'\pi^-$ is dominated by the P_+ and D_+. The common analysis of the observed $\eta'\pi^-$ partial waves gives no preference to the hypothesis of the $\pi_1(1600)$ production.
- We confirmed the results of the $b_1\pi$ analysis of the $37 GeV/c$-beam data. The broad bump has been observed in the $1^-1^+S1(b_1\pi)$ of the $\omega\pi^-\pi^0$. The simultaneous fit with the $2^+1^+S2(\omega\rho)$ favors the existence of a resonance in the $b_1\pi$ with the mass $\sim 1.6 GeV$ and the width $\sim 330 MeV$.
- The PWA of the $37 GeV/c$-beam data sample in the several t' intervals shows a wide bump in the $J^P M^\eta(isobar - bachelor) = 1^-1^+(\rho\pi)$-wave at $M_{\rho\pi} < 2 GeV$ [20].

ACKNOWLEDGMENTS

This is supported, in part, by INTAS-RFBR 97-02-71017, INTAS-RFBR 00-02-16555, RFBR 00-15-96689 grants.

REFERENCES

1. Isgur, N., and Paton, J., *Phys. Rev.*, **D31**, 2910 (1985).
2. Close, F. E., and Page, P. R., *Nucl. Phys.*, **B443**, 233 (1995).
3. Chung, S. U., et al., *Phys. Rev.*, **D60**, 092001 (1999).
4. Abele, A., et al., *Phys. Lett.*, **B423**, 175 (1998).
5. Abele, A., et al., *Phys. Lett.*, **B446**, 349 (1999).
6. Khokhlov, Y., et al., *Nucl. Phys.*, **A663**, 596 (2000).
7. Ivanov, E. I., et al., *Phys. Rev. Lett.*, **85**, 3977 (2001).
8. Dorofeev, V. A., et al., "New results from VES", in *Workshop on Hadron Spectroscopy*, edited by B. T., A. Feliciello, and A. Filippi, Frascati Phys. 15, 1999, p. 999.
9. Beladidze, G., et al., *Zeit. fur Phys.*, **C54**, 235 (1992).
10. Herndon, D. J., Söding, P., and Cashmore, R., *Phys. Rev.*, **D11**, 3165 (1975).
11. Hansen, J. D., Jones, G., Otter, G., and Rudolph, G., *Nucl. Phys.*, **B81**, 403 (1974).
12. Groom, D. E., et al., *Eur. Phys. J.*, **C15**, 1–878 (2000).
13. Orear, J., Notes on statistics for physicists (1958), in UCRL-8417.
14. Sadovsky, S. A., On the ambiguities in the partial-wave analysis of $\pi^- p \to \eta\pi^0 n$ reaction (1991), preprint IHEP-91-75.
15. von Hippel, F., and Quigg, C., *Phys. Rev.*, **D5**, 624 (1972).
16. Hou, S., in this proceedings (2001).
17. Zaitsev, A. M., et al., "Search for exotics in $I^G J^P = 1^-1^-$, 1^-0^- and 0^+2^+ waves", in *CP432, Hadron Spectroscopy: Seventh Internaltional Conference*, edited by S. U. Chung and W. H. J., 1997, pp. 461–470.
18. Chung, S. U., and Trueman, T. L., *Phys. Rev.*, **D11**, 633 (1975).
19. Amelin, D. V., et al., *Phys. Atom. Nucl.*, **62**, 445–453 (1999).
20. Kachaev, I. A., in this proceedings (2001).